

THE DEVELOPMENT OF THE NEXT LINEAR COLLIDER AT SLAC*

RONALD D. RUTH

*Stanford Linear Accelerator Center
Stanford University, Stanford, CA 94309*

ABSTRACT

At SLAC, we are pursuing the design of a Next Linear Collider (NLC) which would begin with a center-of-mass energy of 0.5 TeV and be upgradable to at least 1.0 TeV, and possibly 1.5 TeV. The luminosity is designed to be $10^{33} \text{ cm}^{-2}\text{s}^{-1}$ at the lower energy and $10^{34} \text{ cm}^{-2}\text{s}^{-1}$ at the top energy. In this paper, we discuss the accelerator physics issues which are important in our approach, and also the present state of the technology development. We also review the impact that the SLC has had in the evolution of our basic approach.

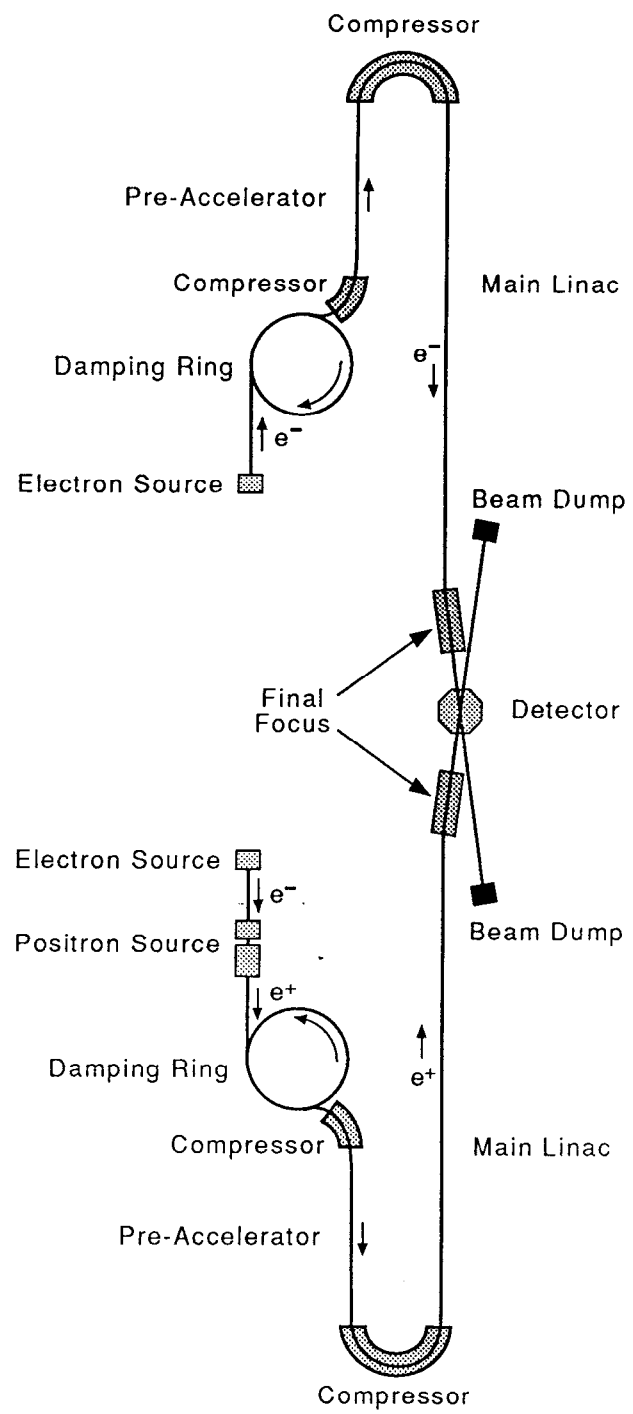
1. Introduction¹

In this paper, we will review the development of the Next Linear Collider (NLC) at SLAC. We are pursuing the design of an NLC which would begin with a center-of-mass energy of 0.5 TeV and be upgradable to at least 1 TeV. The luminosity is designed to be $10^{33} \text{ cm}^{-2}\text{s}^{-1}$ at the lower energy and $10^{34} \text{ cm}^{-2}\text{s}^{-1}$ at the higher energy. Our basic approach is to extend the technology and accelerator physics which is being used for the SLC to the next generation. To obtain the higher energy without excessive length, we choose an RF frequency of 11.4 GHz which is four times the frequency of the SLAC linac. We would like to increase the acceleration gradient to 50–100 MV/m, a factor of three to six beyond the SLC.

To obtain the luminosity without excessive wall-plug power, we focus the beams at the interaction point to a flat ribbon. This controls the beamstrahlung radiation while allowing a small cross-sectional area. The luminosity is further enhanced by the acceleration of many bunches on each cycle of the accelerator.

A possible layout for the NLC is shown in Fig. 1. There are two complete linear accelerators, one for electrons and the other for positrons. Each linac is supplied with particle beams by a damping ring followed by a preacceleration section consisting of two bunch compressors and a 16 GeV linac. After passing through

* Work supported by the Department of Energy, contract DE-AC03-76SF00515.



7-90

4494A96

Fig. 1. Schematic diagram of the NLC.

the main linacs and final focus system, the beams collide at a small crossing angle inside a particle detector.

To illustrate the basic features of the NLC operation, consider the transport of electrons through the collider on a single machine pulse. A train of 10 bunches is created at the source and accelerated to about 1.8 GeV in a preaccelerator. This “batch” of bunches is then injected into a damping ring that serves to reduce the transverse and longitudinal emittance in each bunch. At the proper moment, these bunches are extracted from the ring and compressed along their direction of motion by a bunch compressor, after which they are accelerated to about 16 GeV and compressed a second time just prior to injection into the main, high-gradient, linac. The entire batch is carefully steered and focused as the electrons are accelerated to full energy in the linac. Precision magnets in the final focus system squeeze the bunches vertically by about a factor of 300 just before they collide at the IP with similar bunches of positrons. Except for the fact that the positrons are created differently, from the interactions that occur when a bunch of electrons hits a metal target, their transport is similar to that of the electrons. After the beams collide, their debris is channeled out of the detector area and into shielded dumps.

The parameters for an NLC are not definite yet; however, over the past few years we have narrowed down the range of possibilities considerably. Table I lists three parameter options: the first two columns are for 0.5 TeV in the CM, while the final column is for 1.0 TeV. In Option 1, a relatively short linear collider is constructed with the full accelerating gradient of 100 MV/m. This accelerator can be upgraded to Option 3 by doubling the length of the linac while keeping the injection system fixed. In Option 2, a long linear collider is constructed with a reduced accelerating gradient of 50 MV/m. This can be upgraded to Option 3 by the addition of RF power sources to the linac. In both upgrade paths, the final focus must be modified somewhat. A final upgrade to 1.5 TeV in either case can be obtained by a 50% increase in the length of the linac.

Option 1 has a relatively short linac and may be less expensive than Option 2, but it would require us to face all the problems of the high accelerating gradient and the required high peak power RF sources. In Option 2, we relax the requirements for RF power by a factor of four and begin with a reduced accelerating gradient. The price is an initially longer accelerator with the increased conventional construction.

Before discussing our approach to the design of the NLC, it is useful to review some of the lessons learned from the SLC. After this, we divide the NLC discussion into two sections. The first discusses the accelerator physics and technology necessary to obtain the energy, while the final section focuses on the luminosity.

2. The First Linear Collider: The SLC²

During the past eight years, the first linear collider, the SLC, was constructed and developed at SLAC. This design re-uses the existing linac in a novel way to

Table I. NLC Parameter Options.

Option	1	2	3
Energy	$\frac{1}{4} + \frac{1}{4}$ TeV	$\frac{1}{4} + \frac{1}{4}$ TeV	$\frac{1}{2} + \frac{1}{2}$ TeV
Luminosity	2×10^{33}	2×10^{33}	1×10^{34}
Linac Length	7 km	14 km	14 km
Accel. Gradient	100 MV/m	50 MV/m	100 MV/m
RF Frequency	11.4 GHz	11.4 GHz	11.4 GHz
# Particles/bunch:DR	2×10^{10}	1×10^{10}	2×10^{10}
Linac	1.8×10^{10}	9×10^9	1.8×10^{10}
FF	1.5×10^{10}	7×10^9	1.5×10^{10}
# Bunches, n_b	10	10	10
Beamstrahlung, δ	10%	6%	23%
Repetition Rate	120 Hz	180 Hz	180 Hz
Wall-Plug Power	93 MW	70 MW	280 MW
IP Beam Size: σ_y	4 nm	4 nm	2.5 nm
σ_x	320 nm	200 nm	220 nm
σ_z	100 μ m	100 μ m	100 μ m
$\sigma_{\Delta E/E}$	0.18%	0.18%	0.15%

accelerate the electron and positron colliding bunches, as well as a trailing third bunch which is used to produce the next round of positrons. This technique was possible because at the required energy of about 50 GeV, it is possible to bend e^\pm beams without excess loss of energy or emittance dilution. This led to the characteristic tennis racket shape of the SLC.

In spite of the distinction of a “folded” design, however, the SLC is the technology and accelerator physics base for the Next Linear Collider. During the detailed design and subsequent commissioning and development of the SLC, we have had to face the real issues which limit performance of a linear collider. Many lessons have been learned, in fact, hundreds of articles have been written on the details of designing and operating a working linear collider. In this section we will discuss a few of the highlights from SLC which form the foundation of SLAC’s approach to the NLC.

2.1. Low-Emittance Production

The SLC damping rings were designed to provide very low-emittance electron beams at a high repetition rate (180 Hz). Although the technology and accelerator physics of electron storage rings is well understood, the SLC damping rings were the first designs which combined very low emittance and high repetition rate. The basic design of these rings has been confirmed in practice; they achieve their design asymptotic emittance.

One of the most critical components of the entire collider has turned out to be the damping ring extraction kicker. During SLC development it has been necessary to develop very stable kicker power supplies and also techniques for shaping the pulse of the kicker to vary the kick separately on each of two extracted bunches. This will be especially important in an NLC where trains of 10 or more bunches will be extracted at once.

Damping rings are especially sensitive to the longitudinal impedance seen by the beam as it passes through the vacuum chamber. An excessive impedance causes bunch lengthening and an increase in the relative energy spread of the bunches. The bunch lengthening observed in the SLC damping rings agrees very well with theoretical bunch lengthening using detailed calculations of the damping ring impedance.

Finally, upon extraction from the SLC damping rings, it is necessary to compress the bunch length from about 7 mm to 0.5 mm. This requires a transport line with careful chromatic and dispersive compensation. Although the SLC bunch compressors initially did their compression job very well, they also were responsible for a sizable portion of the emittance dilution. To eliminate this dilution, it has been necessary to develop both linear and nonlinear compensation techniques to match the beam from this complex transport line into the linac to be accelerated.

2.2. Acceleration

This brings us to the heart of any linear collider, the main linac. Although the SLC re-uses the basic accelerator structure and waveguides from the SLAC linac, it was necessary to modify many of the remaining parts of the RF power system and low-power phase control system. New klystrons were developed, which produce 65 MW of peak RF power at 2.86 GHz in pulses 3.5 μ s long. Although at one time these klystrons had their development problems, they are now very reliable and have lifetimes far longer than initially expected. This experience is being directly applied to the development of klystrons for the NLC at 11.4 GHz.

The power level of 65 MW is not sufficient to reach the required acceleration gradient of 17 MV/m. A new device called SLED was invented at SLAC which compresses RF pulses while increasing the peak power up to about 160 MW. This has proved a valuable tool and a new modification, dubbed SLED II, is planned for the NLC.

The phase control requirements and the management of the linac energy profile are much more critical in a linear collider than in a conventional linac. It is necessary to shift the phase of each bunch on the RF wave by a precise amount in order to compensate single-bunch energy spread. The multibunch energy control is provided by matching the rate of extraction of energy to the rate of input. All of the technology, control system and accelerator physics of this acceleration process has been tested in detail in the SLC main linac. The problems in an NLC are very similar to those which have been solved for the SLC; the primary difference is the factor of four higher frequency.

2.3. Emittance Preservation

Acceleration and transport in the main linac can lead to the dilution of the beam emittance. Several developments at the SLC have made it possible to preserve the tiny emittance produced by the damping rings. The routine beam position measurement at SLC is done with a precision of $20 \mu\text{m}$. With these precise measurements, it is possible to control the trajectory of the electron beam at the $50 \mu\text{m}$ level. With this level of precision, beam-based alignment has been used to align the entire SLC linac.

Single-bunch transverse beam breakup can be cured by using a correlated energy deviation (BNS damping). This technique was experimentally tested at the SLC and is part of the normal running configuration. Residual tail growth of the bunches is compensated by deliberate bunch offsets to cancel the growth.

The BNS correlated energy spread is a measure of the relative size of the wakefield forces and the external focusing forces. In the SLC, at design current, the value is several percent. In this case alignment tolerances tend to be the order of the beam size. For the NLC we would like tolerances much larger than the beam size. To do this, it is necessary to have a much smaller BNS energy spread. For the NLC design at SLAC the BNS energy spread is a few tenths of a percent, an order of magnitude smaller than that for the SLC.

While these compensations are necessary to achieve robust stable running, they are not sufficient to prevent drift which causes the beam to deteriorate. This drift is held in check with a sequence of feedback systems which steer the beam to a reference trajectory. For the NLC this puts special emphasis on keeping the repetition rate high enough to provide effective sampling for feedback.

2.4. Matching Diagnostics and Phase Space Certification

In order to match the beam condition to its ideal value, it is necessary to measure beam sizes and lengths rather precisely. In the SLC the beam size measurement is done with wire scanners for beam sizes in the range $1.5 \mu\text{m}$ to $100 \mu\text{m}$. This information is used to adjust compensating magnets in order to precisely

match the beam to its desired size and divergence. In the longitudinal direction it is very difficult to measure the bunch length directly; however, by using a longitudinal energy correlation together with known dispersion, the bunch lengths are measured down to the 0.5 mm minimum bunch length provided by the bunch compressor. This bunch length is adjusted as the intensity is varied in order to achieve the optimum energy spread at the end of the linac. All of these techniques can be directly applied to the NLC.

2.5. Particle Beam Transport

After the beams leave the linac, they are separated and travel through two arcs which lead to the SLC final focus. These arcs are not constructed in a plane and must transport the beam without diluting the emittance. Because of the very strong focusing, the quadrupole magnets are used as correctors by adjusting their position with precision magnet movers. The SLC arcs have provided the first large-scale experience with computer-controlled alignment. In order to compensate errors due to misalignments in the SLC arcs, the 4×4 transport matrices have been completely reconstructed using beam data. This information has been used to successfully compensate the system to bring it to the design performance. This type of compensation may also be necessary to control dilution in the NLC bunch compressor systems.

2.6. SLC Final Focus

Perhaps the first lesson learned about the final focus system is actually upstream of it: in order to operate the detectors, it is necessary to collimate the beams well before they enter the final focus. This process is essential for successful physics runs, and will also be important in an NLC. The tuning of the SLC final focus has taught us how to use beam-beam effects (deflection and beamstrahlung) to optimize the spot size. From time to time, the beams are scanned across each other. This yields the characteristic beam-beam deflection curve which can be used to determine the convolution of the spot sizes as well as the position for head-on collisions. This spot size information is used to adjust the chromatic correction system in order to tune the optics to the matched configuration to achieve minimum spot size. For the NLC designs, we have learned the importance of separating the functions of phase-space matching from the final focus system. We have also learned the importance of detailed tuning strategies, lessons which are already being applied to the design of the Final Focus Test Beam (see Section 4.8.).

2.7. System Issues

Some of the most important lessons learned thus far from SLC experience are also the most difficult to quantify; these can be loosely termed “system issues.” Qualitatively, as a system, an electron storage ring is rather like a damped

pendulum. It has a stable configuration which is only perturbed adiabatically if parameters vary. The system is perturbed every now and then for injection, but in all other aspects it is a steady-state system.

In a linear collider, the beam is recreated on each cycle of acceleration. The electrons remember their initial conditions and all downstream parameters are affected by changes upstream. As a system the linear collider behaves rather like a pencil balanced on your finger tip. In order to keep the balanced pencil stable it is necessary to provide feedback at the base. For the linear collider, feedback is the key to stable operation. It must deal with changes every 10 pulses or so as well as day/night drift due to small temperature changes.

The stable operation of the system is also coupled tightly to the overall complexity and the reliability of individual components. In order to provide sufficient time for stable running, it is necessary to eliminate tuning of the linear chain of components. High reliability and stability help reduce this to a minimum. In a complex system such as a linear collider, one cannot expect peak performance from all systems simultaneously. For reliable operation, experience at SLC indicates that a significant margin is required in each system.

3. Obtaining The Energy

3.1. *The Basic Approach*

The energy for the NLC is obtained by a combination of length and acceleration gradient. At SLAC, we have chosen to push acceleration gradients a factor of three to five up to 50–100 MV/m. In order to accomplish this while still controlling the wall-plug power, we increase the frequency by a similar factor up to 11.4 GHz. Other than this change, the NLC RF system is modeled after the successful SLC RF system. A schematic of the system is shown in Fig. 2. The RF power flows from the source through waveguides to a travelling wave structure. After the structure is full, the beam is accelerated and the remaining energy flows out of the structure into a cooled load. Perhaps the best place to begin the discussion of the NLC RF system is at the RF structure.

3.2. *The RF Structure*

The RF structures planned for the NLC are rather similar to those presently being used at the SLC except for the factor of four change in frequency. The basic parameters are shown in Table II. The key difference is a modification in design to reduce the transverse wakefields induced by bunches which are offset in the structure. First, in order to control the wakefield within a bunch, the iris holes have been increased by about a factor of two relative to the wavelength. Although this slightly increases the required power, the short-range transverse wakefield is reduced by about an order of magnitude by this simple modification. Second,

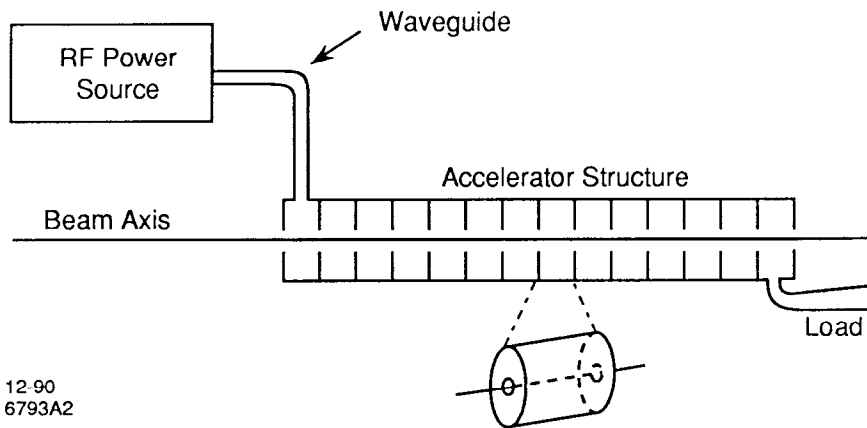


Fig. 2. Schematic of the NLC RF system.

Table II. NLC Structure Parameters

Section Length	L_s	1.8 m
Beam Aperture Radius	$\frac{a}{\lambda}$	0.175
Group Velocity	$\frac{v_g}{c}$	0.06
Filling Time	T_f	100 ns
Unloaded Time Constant	T_o	198 ns
Attenuation Parameter	τ	0.505
Elastance	s	815 V/pC/m
Structure Efficiency	η_s	0.629
Peak Input Power/Meter at 50 MV/m	\hat{P}_m	49 MW/m
Peak Power per Feed at 50 MV/m	\hat{P}_{feed}	88 MW
Structure Average Power Dissipation at 50 MV/m*	\bar{P}_{str}	840 W/m

*150 ns at 180 pps.

because it is necessary to accelerate many bunches during each machine cycle to achieve the desired luminosity, the structure must also be modified to reduce the

long-range transverse wakefield.

This can be accomplished by two techniques. In the first method, the cavity design is altered so that the deflecting fields are strongly coupled to external waveguides. After a bunch passage, the fields in the structure die out quickly as they propagate out the waveguide into a matched load. The second technique relies on the cancellation of the deflections from cell to cell. If the cells in a single structure are designed so that the deflecting modes oscillate at different frequencies, then the average deflection over the structure effectively damps due to the decoherence of the various cell wakefields.

Both techniques have been theoretically studied and experimentally tested at SLAC.^{3,4} Present designs at SLAC are focusing on the "detuned" option due to its simplicity. An experimental test of this technique is shown in Fig. 3, together with theoretical estimates of the wakefield for a model detuned structure. This model used a Gaussian distribution of frequencies for the higher-order modes, but the effect was exaggerated in a structure with a small number of cells. The experiment was a success and showed excellent agreement with theory.

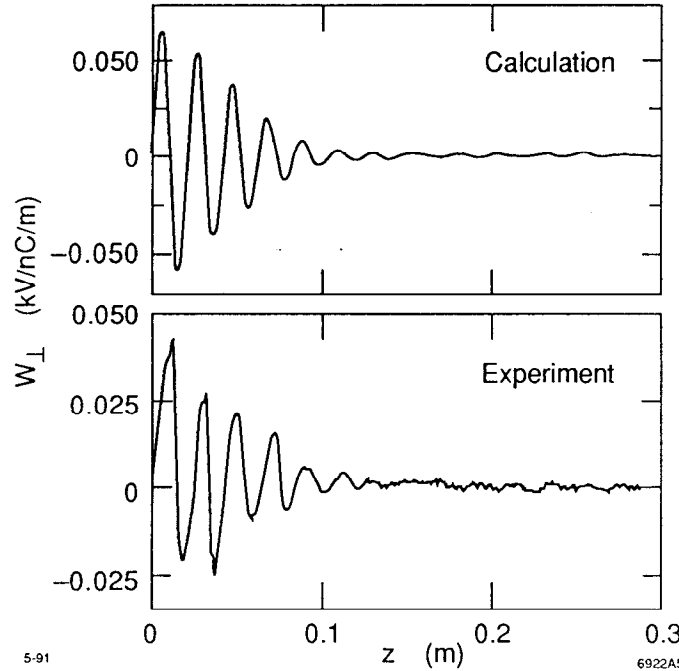


Fig. 3. Transverse wake potential for the HEM₁₁-detuned 50-cavity disk-loaded structure. Top: calculation by LINACBBU ($\sigma_z = 0$). Bottom: Measurement result at AATF ($\sigma_z \approx 2.5$ mm).

The actual structure will have a Gaussian distribution in the higher-order modes which is tailored by adjusting the cell dimensions while keeping the funda-

mental accelerating mode frequency constant. This structure is reminiscent of the SLC structure which is modified in a similar way to create a constant gradient. The calculated wakefield of this structure is shown in Fig. 4, and the variation of accelerating field along the structure is shown in Fig. 5. Structures with this wakefield yield less than 10% blowup bunch-to-bunch in an NLC. We plan to begin construction of a full-scale detuned structure in 1992.

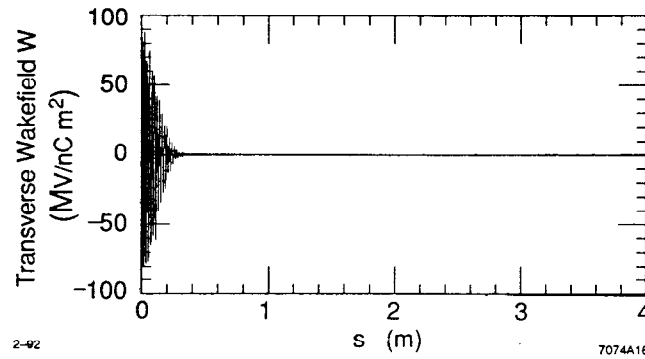


Fig. 4. The transverse wakefield of the detuned structure.

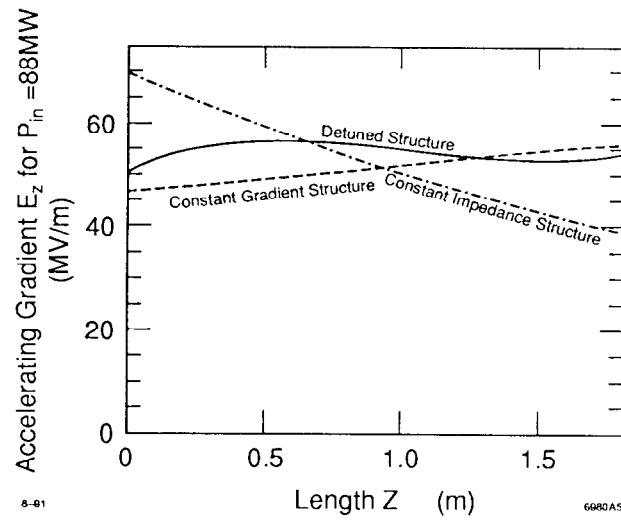


Fig. 5. Variation of accelerating field along the detuned structure.

In order to verify that it is possible to reliably accelerate beams with gradients in the range 50–100 MV/m, we are conducting high-power experiments with model structures. The latest high-field test was conducted on a seven-cell, 11.4-GHz standing wave structure. Although the peak field reached was limited by the available input power, the structure was powered to peak surface fields in excess of 500 MV/m. This would correspond to a travelling wave accelerating field of about 200 MV/m.

High-power tests in 1992 will include a 30-cm-long structure and a 75-cm-long structure. The focus of these experiments will be on the generation of dark current due to field emission. Early indications are that the dark current will not be a problem at 50 MV/m, but may cause problems for acceleration gradients in excess of 100 MV/m.

3.3. The RF Power System

The elements of the NLC RF power system are shown in Fig. 6. The RF power is supplied by a klystron amplifier. In order to obtain the correct pulse length and peak power, this RF pulse is compressed by about a factor of six by an RF pulse compression system. The overall system is supplied by a modulator (pulsed power supply). The primary goal for the system is to provide RF power with the correct peak power and pulse length as efficiently as possible.

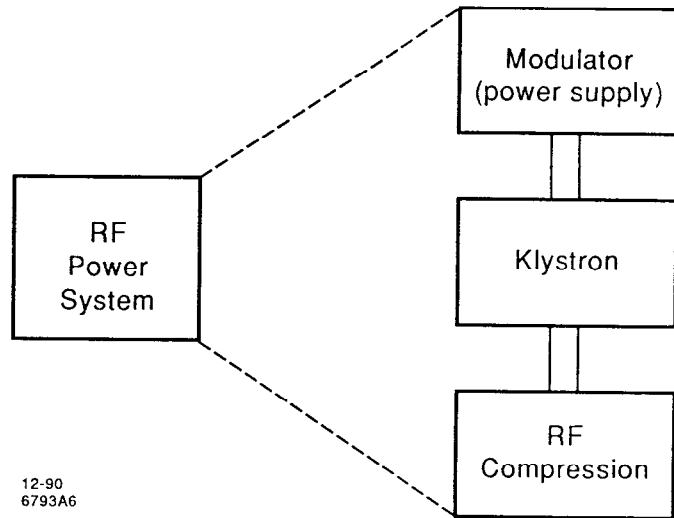


Fig. 6. Elements of the NLC RF system.

3.4. RF Pulse Compression

The object of RF pulse compression is to convert a long RF pulse of moderate power into a short RF pulse with high power. Ideally, a factor of five decrease in pulse length could yield a factor of five increase in peak power. Due to inefficiencies, the factor is always somewhat less. The RF pulse compression system SLED (SLAC Energy Development) is presently used at SLAC to boost the klystron power by about a factor of three before powering the SLAC linac. This system uses storage cavities to allow the RF to build up. A phase switch from the klystron causes the klystron power and the power emitted from the cavity to add coherently, yielding a narrow pulse of high peak power. Unfortunately, this system gives a pulse shape which is sharply spiked due to the exponential decay of the fields in the storage cavities. For an NLC it is useful to have a flat-top pulse to control multibunch energy spread.

This flat-top pulse can be obtained by two different methods. The first method, called binary pulse compression (BPC), uses delay lines to delay the leading portion of an RF pulse so that it is coincident in time with the trailing portion. This yields an RF pulse which is one half as long, but with nearly twice the power. This process can be repeated in a sequence to achieve more and more multiplication. Due to losses in components and waveguides, the method is limited to about three compressions.

Figure 7 shows a schematic diagram of a two-stage BPC system which was constructed at SLAC.⁶ The 3-db hybrid shown in Fig. 7 is a four-port device which combines two power inputs into one or another output port depending upon relative phase. In this way phase shifts can be used as high power RF switches. A three-stage system of analogous design has been constructed at SLAC and has achieved a multiplication factor of 5.5 while reducing the pulse length by a factor of eight.⁷ This system, together with new high-power klystrons, is used to test the RF structures described above.

2 STAGE BEC SCHEMATIC

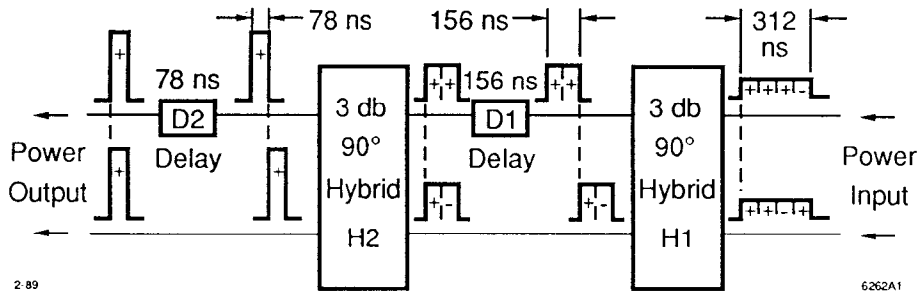


Fig. 7. Schematic diagram of a BPC system.

One disadvantage of the BPC method of pulse compression is that it uses

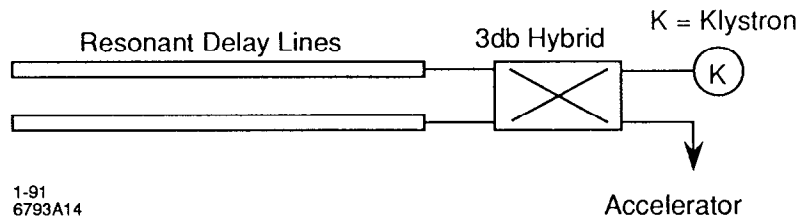


Fig. 8. A block diagram of SLED II.

rather long delay lines. The waveguides which are used have a group velocity very close to the speed of light, and they are only used once as transmissive delay lines. This problem has led to the development of a new pulse compression scheme called SLED II.⁸ The system as shown in Fig. 8 is similar to the SLED system at SLAC except that the cavities for storing the RF are replaced by resonant delay lines. Each of these delay lines has a round-trip delay time equal to the output pulse length. A resonant buildup of energy stored in the lines takes place during an input pulse length which is an integral number of delay periods, typically in the range of four to eight. A phase reversal of the input pulse effectively triggers the compression to produce a flat-top output pulse during the final delay period. An example of a SLED II pulse compression by a factor of four is shown in Fig. 9. Measurements from a low-power SLED II system with a power gain of four have shown excellent agreement with theory.

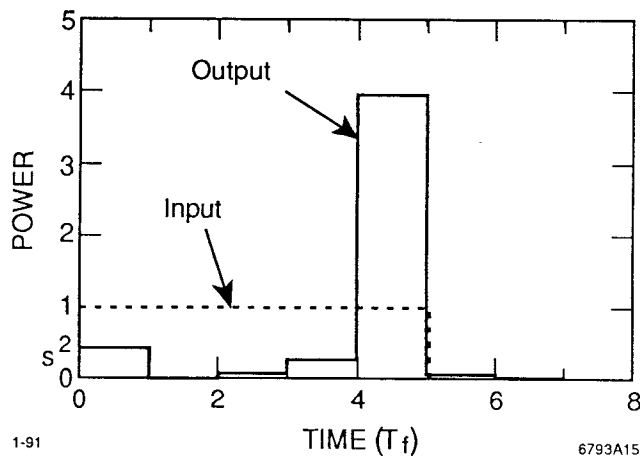


Fig. 9. SLED II pulse compression.

Comparing SLED II with BPC, the amount of waveguide delay line to achieve a similar compression is reduced by about a factor of five. This is due to the

reflective nature of the scheme; the delay lines are used repeatedly as the RF wave builds up. In addition, this method can be staged by placing the SLED II systems in series to provide even larger compressions if necessary. A high-power SLED II pulse compression system will be constructed at SLAC in 1992 to investigate this promising technique further.

3.5. The Klystron⁹

Although a 50-MW klystron would probably suffice for a 500-GeV linear collider, the goal for klystron development at SLAC is to produce a reliable and efficient 100-MW, 11.4-GHz klystron with a pulse length of about 1 μ s. The designs of these klystrons are based on the successful experience with 65-MW SLC klystrons during the past eight years. There are a few differences due to the higher power and frequency. The solenoidal field which confines the klystron beam is increased to decrease the beam size transversely. The beam energy is increased and the electric fields at the output are increased due to the smaller wavelength. A summary of klystron performance thus far is shown in Fig. 10. The third klystron, XC3, reached power levels similar to those reached by XC2.

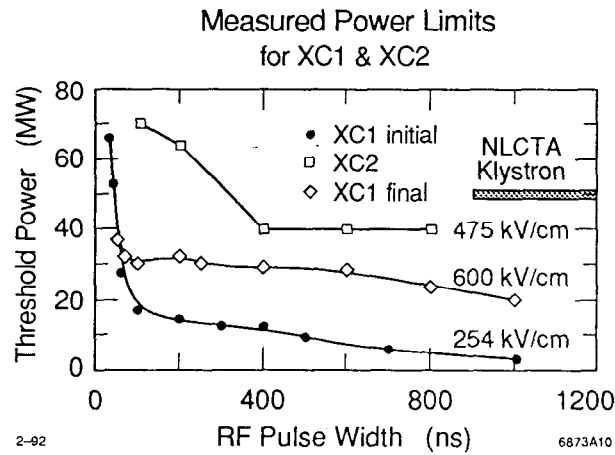


Fig. 10. Summary of klystron performance.

The problems which have thus far limited performance are related to the high power and high frequency. These are RF breakdown at the output cavities, beam optics, beam erosion and window reliability. Each of these problems is being addressed in new designs which will be tested in 1992. We hope, by the end of 1992, to have a reliable 11.4-GHz klystron which produces more than 50 MW in a pulse about 1 μ s long.

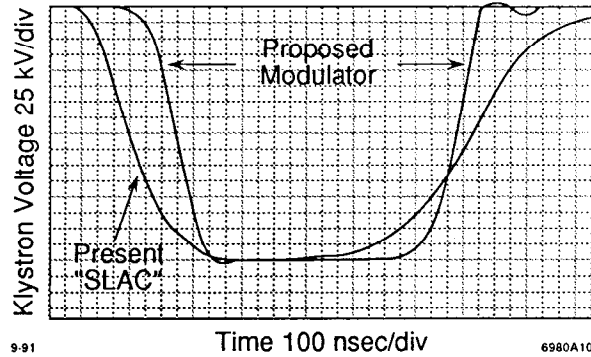


Fig. 11. Output pulse shape for new modulator design.

3.6. The Modulator

The modulator is a critical component in an NLC due to its impact on cost and efficiency. The challenge is to produce a beam voltage pulse in the range of 400–600 kV for about 1 μ s with a rapid rise time to enhance efficiency. Conventional SLAC-type modulators have slow rise times due to the 20:1 turns ratio of the transformer. A new design developed at SLAC¹⁰ uses a multiplying Blumlein pulse-forming network which allows a reduction in the turns ratio of the pulse transformer to about 6:1. The output pulse shape for this new design is compared with the present modulator pulse in Fig. 11. The improved rise time and a substantial gain in efficiency are evident from the figure. This new design will be tested in 1992 by converting one of our present klystron test stands to the new design.

3.7. The NLC Test Accelerator

The previous sections have discussed the status and plans for the RF system and accelerating structure for an NLC. In order to integrate these separate development efforts into an actual X-band accelerator capable of accelerating e^- beams necessary for an NLC, we propose to build an NLC Test Accelerator (NLCTA). The goal of the NLCTA is to bring together all the elements of the entire accelerating system to construct and reliably operate an engineered model of a section of a high-gradient linac suitable for the next linear collider. The NLCTA will serve as a test bed as the design of the NLC evolves and will provide a model upon which a reliable cost estimate of an NLC could be based. In addition to testing the RF acceleration system, the NLCTA will be able to address many questions related to the dynamics of the beam during acceleration.

3.7.1. Basic Parameters

The NLCTA consists of a high-gradient X-band linac injected by a simple

Table III. NLCTA Parameters

Energy	540 MeV	(1280 MeV)
Linac Length	15 m	
Accelerating Gradient, \mathcal{E}_z	50 MV/m	(100 MV/m)
Injector Energy, E_o	100 MeV	
RF Frequency, f_{rf}	11.42 GHz	
Number of Klystrons	3	(6)
Klystron Peak Power	50 MW	(100 MW)
Klystron Pulse Length	0.9–1.2 μ s	
RF Pulse Compression	4.0	
Structure Type	2 π /3 Detuned	

thermionic gun and followed by a spectrometer to analyze the accelerated beam. A schematic layout is shown in Fig. 12 and the parameters are listed in Table III.

The NLCTA will be injected by a simple thermionic gridded gun which will be followed by an X-band prebuncher cavity. A very minor modification of one X-band accelerator section converts it to a capture section for the X-band linac. The X-band linac consists of six accelerator sections (each 1.8 m long). These sections are fed (in the initial phase) by three 50-MW klystrons which make use of SLED-II pulse compression to increase the power by a factor of four. This yields an acceleration gradient of 50 MeV/m so that the total energy gain in the X-band linac is 540 MeV. After acceleration, the bunch train will be analyzed to determine energy and energy spread. We will also plan to measure beam emittance and transverse offsets along the bunch train.

The right-most column of Table III lists the parameters for an upgrade of the X-band linac to 100 MV/m by the use of six 100-MW klystrons. Although the initial proposal does not include this upgrade, this is one possible path to 100 MV/m in the NLCTA.

4. Obtaining The Luminosity

In the Introduction and in Section 3, we discussed the basic layout and how to obtain the energy in a linear collider; in this section, we discuss how to obtain the luminosity. Although the luminosity depends upon beam properties at the interaction point, those properties depend upon beam dynamics throughout the entire linear collider; therefore, we must trace this influence throughout the collider. Before doing that, however, let's examine the luminosity formula. Luminosity for a

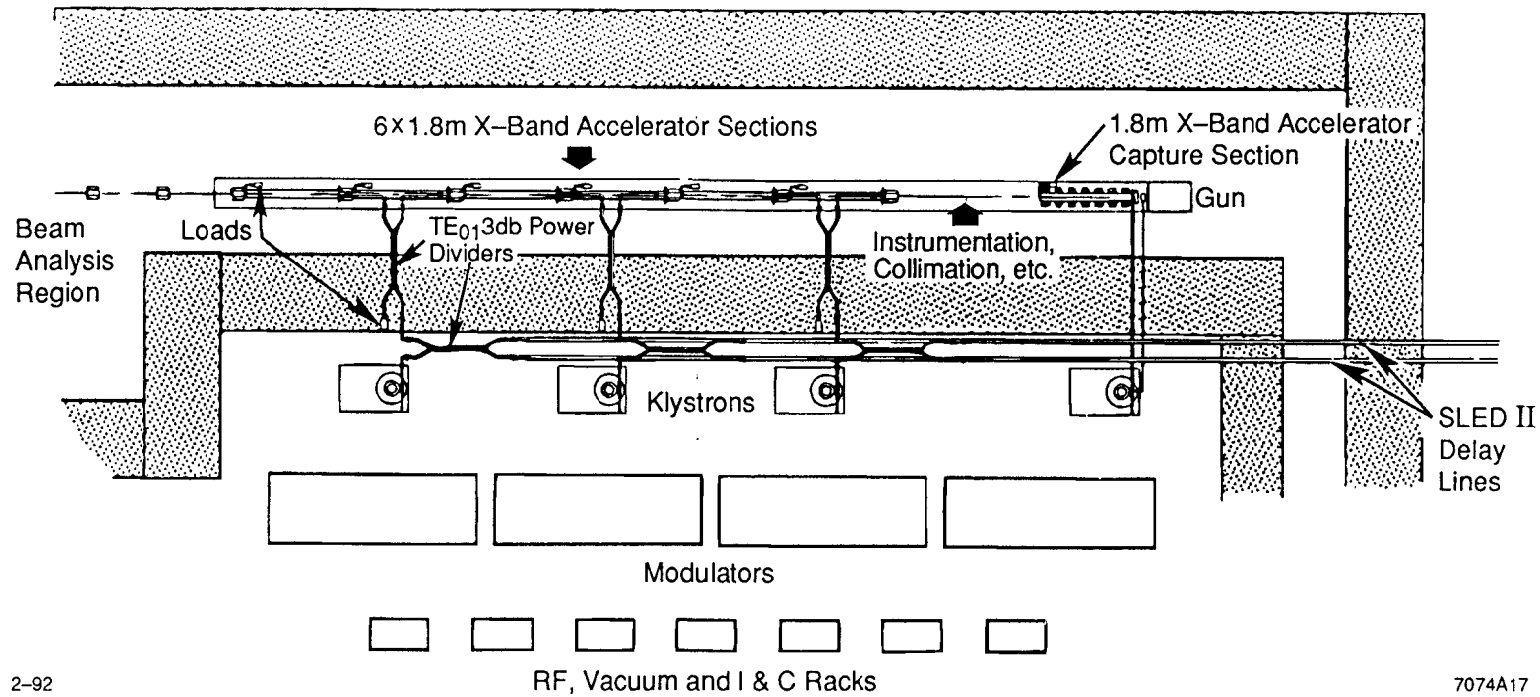


Fig. 12. NLC Test Accelerator.

linear collider is the same as for a circular collider except that there is an additional term, an enhancement factor due to the mutual pinching of the beams. The luminosity is given by

$$\mathcal{L} = \frac{N_+ N_- f_{rep} n_b}{4\pi\sigma_x\sigma_y} H_D , \quad (1)$$

where N_{\pm} is the number of positrons/electrons per bunch, f_{rep} is the repetition frequency, n_b is the number of bunches accelerated on each cycle of the accelerator, H_D is the pinch enhancement factor, and finally, σ_x and σ_y are the rms beam size of the gaussian spot at the interaction point. Each bunch is assumed to collide with only one other bunch in the opposing bunch train.

The object is to increase the luminosity to 10^{33} – 10^{34} cm $^{-2}$ s $^{-1}$, for the energy range $\frac{1}{2}$ to 1 TeV. To do that we must increase the numerator of Eq. 1 and decrease the denominator as much as possible. For the numerator, we have at our disposal the number of particles per bunch, the repetition rate, and the number of bunches on each cycle, but we must satisfy the constraint that the wall-plug power is in the range of 100–200 MW. For the denominator, we can decrease the cross-sectional area by decreasing σ_x and σ_y , but to do this we must keep the beam flat to control beamstrahlung.

In the next few sections we discuss each term in the luminosity formula. The discussion of beam size is subdivided into several sections. In the next section we begin with the numerator of Eq. 1.

4.1. Intensity and Repetition Rate

First let's discuss the single bunch intensity N_{\pm} and the repetition rate f_{rep} . From conservation of energy, we must have

$$NE_{cm}f_{rep} = \eta_{rf}\eta_b P_{wall} , \quad (2)$$

where η_{rf} is the efficiency for converting wall-plug power to RF power, η_b is the fraction of the energy extracted by a single bunch, and P_{wall} is the total wall-plug power supplied to the linacs. The wall-plug-to-RF efficiency, η_{rf} , is about 20% for the projected RF system. This is a fairly realistic estimate including all of the factors in the power system which were discussed in the first section. There are new ideas which could raise this to perhaps 30–40%, however, with the system shown in Section 3.3, η_{rf} is about 20%.

For somewhat different reasons, the single-bunch extraction efficiency is limited to about 2%. The single-bunch beam loading causes an energy spread within

the bunch. Although the linear part can be compensated by shifting the RF phase to obtain a linear slope, the higher order effects are difficult to compensate. However, very small energy spread is required to keep the beam emittance from increasing, to focus the beam to a small spot, and finally, to provide a narrow spectrum for experiments. This limits single bunch energy extraction to a few percent.

For the purpose of this discussion, let's select a wall-plug power of 150 MW for an $E_{cm} = 1$ TeV.

Because the required bunches have a very small transverse dimension, it is necessary to control their offset pulse-to-pulse with a feedback system. In order for this feedback system to work efficiently, the sample rate must be at least six times the rate at which the beam centroid is changing. Because ground motion is an important source of bunch motion, and because the spectrum drops off rapidly above 10 Hz, the repetition rate of the accelerator must be greater than 60 Hz. Experience at SLC has shown that a simple factor of six is not sufficient. A substantial overhead in the sample frequency is required in order to avoid excessively amplifying the high-frequency ground motion. Therefore, we set the repetition frequency to 180 Hz. It could be dropped as low as 120 Hz; however, 60 Hz is probably too low. Substituting the previous parameter values in Eq. 2, we find that the maximum number of particles per bunch is $N_{\pm} \simeq 2 \times 10^{10}$.

4.2. The Number of Bunches

As discussed in the Introduction, the designs for the NLC include the acceleration of many bunches on each cycle of the collider. The purpose of this is, of course, to increase the luminosity linearly with increasing number of bunches. If there were no constraints, the largest luminosity would be obtained by placing all the charge in the bunch train into one bunch because in this case there is quadratic gain with increasing intensity. As discussed in the previous section, the single bunch intensity is limited by the amount of energy it can extract while retaining a small relative energy spread. It turns out that this intensity is also consistent with transverse stability and with beam-beam effects. Thus, the quadratic gain is stopped by these bounds; however, since there is about 98% of the energy left in the structure, it is possible to continue to gain linearly by increasing the number of bunches.

A large number of bunches brings along a host of other complications. Some of these were discussed earlier. The bunches must be stable transversely which means that the structure must be designed in a special way (Section 3.2). The energy spread bunch-to-bunch must be controlled. This can be done by delaying the filling of the RF structure and by matching the rate of filling of the structure to the rate of energy extraction. This technique is used routinely at the SLC. However, as the number of bunches increases, higher-order effects become important and the compensation technique becomes more difficult. This limits the number of bunches to about 10; although the single bunch intensity can be traded off somewhat with the number of bunches. There are other strategies for bunch-to-bunch energy

compensation which allow larger energy extraction; however, because of the heavier beam loading, the tolerances are much tighter.

The RF pulse must be of rather high quality. Systematic phase and amplitude variations over the bunch train must be less than about 2% (such tolerances are not unrealistic with the power sources discussed). Because a significant fraction of the fields felt by the trailing bunches are due to the leading bunches, the intensity of the bunch train must be controlled with a precision less than 2%. The damping rings which produce these trains of bunches must be able to accelerate them without instability. If small position or energy changes occur, a compensation system must be developed to assure that the bunches enter the final focus system on the same trajectory and with the same energy. The final focus system must be designed so that the distant crossings of bunches do not disrupt the primary collisions at the interaction point.

Although the addition of many bunches appears to be “free” in that we simply use energy that would normally be wasted, it introduces complexity into every subsystem of the entire collider. The benefit is an order of magnitude increase in the luminosity.

4.3. The Beam Size

The transverse size of a beam in an accelerator is determined by two basic parameters: the emittance ϵ and the beta function β ,

$$\sigma = \sqrt{\epsilon\beta} . \quad (3)$$

The emittance is a parameter that is proportional to the area occupied by the beam distribution in transverse phase space (x, p_x) . It is defined by

$$\epsilon_x = \frac{1}{p_0} [\langle x^2 \rangle \langle p_x^2 \rangle - \langle xp_x \rangle^2]^{\frac{1}{2}} , \quad (4)$$

where x is the transverse position, p_x is the corresponding transverse momentum, and p_0 is the central momentum of the bunch of particles. The angle brackets in Eq. 4 indicate an average over the distribution of particles in a bunch. Because the quantity in the square brackets is an adiabatic invariant (in the absence of synchrotron radiation), the emittance decreases inversely with the momentum of the bunch in a linear accelerator.

The longitudinal emittance is defined in a similar way,

$$\epsilon_z = \frac{1}{p_0} [\langle z^2 \rangle \langle \Delta p^2 \rangle - \langle z \Delta p \rangle^2]^{\frac{1}{2}}, \quad (5)$$

where z is the longitudinal deviation from a central position within the bunch, and Δp is the deviation of the particle momentum from a central momentum. Once again, the quantity in the square brackets is an adiabatic invariant, which causes ϵ_z to decrease inversely with the beam momentum in a linear accelerator. In the special case of a high-energy electron linac, the longitudinal distribution and the bunch length are fixed because the particles all travel at essentially the speed of light. In this case, the fractional momentum spread varies inversely with the beam momentum.

The beta function β was first introduced by Courant and Snyder in their description of the alternating gradient focusing of particle beams.¹¹ The parameter not only determines the particle beam size through Eq. 3, it also determines the instantaneous wavelength of the oscillations of particles within the beam envelope as they traverse the focusing magnets (wavelength = $2\pi\beta$).

The beta function also plays an important role at the interaction point (IP). In a magnet-free region, it has the particularly simple form

$$\beta(s) = \beta^* + \frac{(s - s_0)^2}{\beta^*}, \quad (6)$$

where β^* is the minimum value of $\beta(s)$ and s_0 is the location of that minimum, the IP in this case. According to Eq. 3, the beam size near the IP is therefore

$$\sigma^2(s) = \epsilon\beta^* + \frac{\epsilon}{\beta^*}(s - s_0)^2. \quad (7)$$

From this form, it is obvious that β^* is the depth of focus because the beam size increases by $\sqrt{2}$ when $s - s_0 = \beta^*$. Thus, the beta function plays two important roles at the IP—it determines both the spot size and depth of focus. In order to achieve the sizes shown in Table I, we must reduce the emittance as much as possible and preserve it during acceleration, and finally, we must focus the beam down to provide a small β^* at the interaction point.

4.4. The Damping Ring^{12,13}

The damping ring serves to reduce the emittance of the bunches of particles in all three degrees of freedom. It is an electron storage ring similar in all essential

features to the storage rings used for colliding beams or synchrotron light production. The particles in an electron storage ring radiate a substantial fraction of their energy on each turn—energy that is restored by RF accelerating cavities. In the process of radiation, the particles lose energy from all three degrees of freedom, but it is restored only along one, the direction of motion; the proper amount is supplied at a single RF phase for a particle with the design energy, which leads to damping in all three dimensions. The fact that radiation is emitted as discrete quanta, however, introduces stochastic noise that causes diffusion of particle trajectories.

The competition between these damping and diffusion effects leads to an equilibrium value for the emittance of an electron storage ring. Damping rings are designed to enhance the damping effects using strong magnetic fields (such as those in wiggler magnets), while limiting the diffusion by the special design of the transverse focusing in the ring. In addition, there is a unique feature of electron storage rings that can be used to advantage. Due to the lack of vertical bending, the vertical emittance of the beam is much smaller than the horizontal—typically two orders of magnitude smaller. Such naturally flat beams are a key feature of many NLC designs.

One possible design for a future damping ring is about a factor of five larger and operates at an energy 50 percent higher than that of the SLC damping rings (see Fig. 13). The final emittance of the beam is more than an order of magnitude smaller than that of the SLC beams, which leads to much smaller sizes. In fact, the vertical extent of a beam emerging from this damping ring would be a few microns, or about equal to the final spot size at the SLC interaction point.

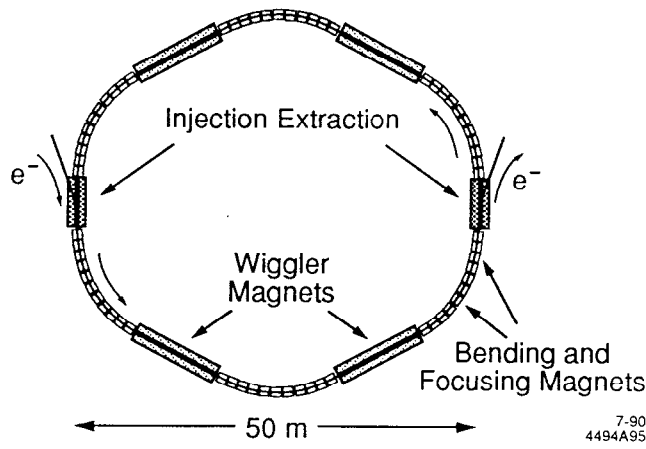


Fig. 13. A design of an NLC damping ring.

Another key difference is the simultaneous damping of many batches of bunches. In the SLC, at most two bunches are damped simultaneously, whereas

this NLC ring will damp 10 batches of 10 bunches all at once. This feature allows a longer damping time for any given bunch, because we can extract the “oldest” batch and inject a new “young” batch while leaving those in their “adolescence” to continue damping undisturbed.

Because the bunches forget their origins in the damping ring, their conditions upon emerging are entirely determined by their behavior in the damping ring. This places special emphasis on the stability of the magnets in the damping ring and extraction system.

4.5. Bunch Compression/Pre-Acceleration^{14,15}

Although the longitudinal emittance obtained in the damping ring is small enough, the bunch is still much too long for acceleration in a linac. In the SLC and NLC, this problem is solved by a technique called bunch compression, which shortens the bunch while increasing its energy spread. Each bunch passes through an RF accelerating structure phased so that the trailing particles emerge with lower energy than the leading particles. Then the bunch passes through a sequence of magnets that disperses the beam so that particles of different momenta travel on different paths. Particles with higher momentum (at the head of the bunch) travel a longer path than those of lower momentum (at the tail). The tail of the bunch can therefore catch up with the head, producing a shorter bunch—but at the cost of a greater energy spread.

This type of bunch compression has been used routinely in the SLC, where bunches 7 mm long are compressed to 0.5 mm for acceleration in the linac. Much shorter bunches will be required in the NLC. Short bunches will suffer less from transverse wakefields in the linac, and they permit a smaller depth of focus at the IP (about 100 microns for the NLC). In principle, another order of magnitude in compression could be obtained in a single stage; in practice, however, this approach would lead to other deleterious effects due to the large energy spread that would be induced in the beam. For this reason, the extra compression is provided by a second bunch compressor operating at a higher energy.

In the NLC, the bunch is first compressed as in the SLC to 0.5 mm in length, after which the beam is accelerated to about 16 GeV. The longitudinal spread of the beam is unaffected by this acceleration, but the relative energy spread decreases linearly with energy. The compression is then repeated, resulting in a bunch length less than 100 microns. By separating the compression process into two discrete steps, we can keep the relative energy spread small throughout.

4.6. Emittance Preservation During Acceleration¹⁸

During the process of acceleration, we must take care not to dilute the emittance of the beam. There are several effects which can lead to emittance dilution. In the next few subsections, we discuss a few of the most important effects.

4.6.1. Chromatic Effects

The filamentation of the central trajectory in a linac can cause dilution of the effective emittance of the beam. If we first consider a coherent betatron oscillation down the linac, then to be absolutely safe, we must require that it be small compared to the beam size. If the spread in betatron phase advance is not too large, then this tolerance is increased to perhaps twice the beam size for the design shown in Table I.

The chromatic effect of a corrected trajectory is rather different. In this case, it is the distance between an error and a corrector which matters, and the effects partially cancel yielding a growth $\propto \sqrt{N_{quad}}$. This yields a tolerance on magnet misalignment the order of 20 to 30 times the beam size in the linac (about 20 μm) for the design in Table I. This is also the tolerance on BPM accuracy. If the phase advance of the linac or some subsection is not too large, then this yields a linear correlation of position with momentum (dispersion) which can, in principle, be corrected since it does not vary in time. Therefore, it is possible to have looser tolerances if such correction is provided.

4.6.2. Correction Techniques

As the trajectory is corrected the dispersion grows. It is possible, however, to measure this effect and choose a trajectory which is small and also has small dispersion. This type of compensation technique has been extensively investigated.^{16,17} If this correction is provided, then normal alignment tolerances (100–200 μm) can be compensated to yield negligible dilution of the beam emittance. For these techniques to work effectively, it is important that the single-bunch wakefields and beam loading be reasonably small.

4.6.3. Transverse Wakefields and BNS Damping

The wakefield left by the head of a bunch of particles, if it is offset in the structure, deflects the tail. If the transverse oscillations of the head and tail have the same wave number, the tail is driven on resonance. This leads to growth of the tail of the bunch.¹⁹ This effect can be controlled by a technique called BNS damping.²⁰ The bunch is given a head-to-tail energy correlation so that the tail is at lower energy. The offset of the head by an amount \hat{x} induces a deflecting force on the tail away from the axis. The tail, however, feels an additional force $\Delta K \hat{x}$, where ΔK is the difference in focusing strength due to the energy difference. These two forces can be arranged to cancel, thereby keeping the coherence of the bunch as a whole. For the designs shown in Table I, the spread in energy for BNS damping is much less than 1%. This correlation can be accomplished by moving the bunch slightly on the RF wave to obtain a linear variation across the bunch. BNS damping has been thoroughly tested at the SLC and is now part of normal operating procedure.

4.6.4. Jitter

In order to maintain collisions at the interaction point, the bunch must not move very much from pulse to pulse. Since the optics of the final focus also demagnify this jitter, the tolerance is always set by the local beam divergence compared to the variation of some angular kick. The jitter tolerance on the damping ring kicker is thus related to the divergence of the beam at that point. At the injection point to the linac, the offset caused by this jitter must be small compared to the local beam size.

If all the quadrupoles in the linac are vibrating in a random way, the effects accumulate down the linac and the orbit offset grows $\propto \sqrt{N_{quad}}$. This sets the tolerance on the random motion of quadrupoles to be much smaller than the beam size. In the examples in Table I, the random jitter tolerances are $\simeq 0.01\mu\text{m}$. However, this size motion from pulse-to-pulse is unlikely due to the large repetition rate of the collider. More gradual motion, which is larger, can be corrected with feedback, provided the repetition frequency is sufficiently large.

Jitter in RF kicks can cause similar effects. These effects can be reduced by reducing the DC component of the RF kick by eliminating asymmetries in couplers and by careful alignment of structures.

4.6.5. Coupling

Finally, we discuss coupling of the horizontal and vertical emittance. The beam size ratio in the linac is 10:1. The tolerance on random rotations for a flat beam is given by

$$\Theta_{rms} << \frac{\sigma_y}{\sigma_x} \frac{1}{\sqrt{2N_q}} \quad . \quad (8)$$

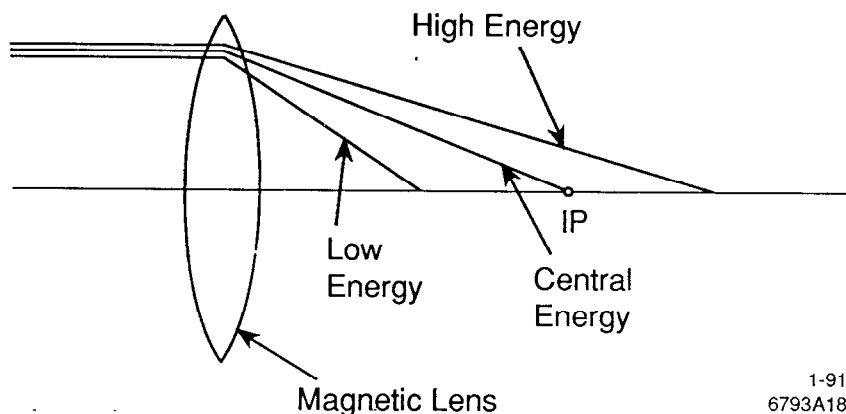
For the example shown in Table I, the right-hand side is about 3 mrad; this is straightforward to achieve. If the errors are not random, larger rotations can indeed result; however, because the beam size is so small, the effects are very linear. This means that skew quadrupoles can be used effectively as correction elements. Certainly, in the final focus, skew quads will be an integral part of the tuning procedure to obtain flat beams.

*4.7. Final Focus*²¹⁻²⁴

At the end of each linear accelerator is a final focus system whose purpose is to compress the tiny bunches to sub-micron dimensions. To obtain the luminosity desired, the cross-sectional area of each bunch must be only a few hundred square nanometers. In addition, we must focus it to the shape of a flat ribbon (rather than a string) in order to minimize the radiation emitted as the particles in the bunch encounter the intense electromagnetic field of the opposing bunch. These

goals are accomplished by the use of a magnetic focusing system analogous (in reverse) to an optical telescope used to magnify distant objects. This system uses quadrupole magnets as focusing elements in a combination that provides a very large demagnification.

A major problem is the so-called "chromatic" effect of the final quadrupole magnets. Two parallel electron beams with different momenta entering a perfect quadrupole magnet are brought to a focus at slightly different longitudinal positions because the lower energy beam is bent slightly more than the higher energy beam by the magnetic field (see Fig. 14). For it not to affect the spot size, this shift of focal point must be smaller than β^* , the depth of focus of the beam. Due to the requirement of flat beams, this depth of focus is about 100 microns in the vertical dimension.



1-91
6793A18

Fig. 14. The "chromatic" effect of the final quadrupole focusing magnet. Particles of differing energy are focused to different locations.

Such a small depth of focus makes the chromatic effects particularly serious. The chromatic correction of the final quadrupoles is in fact the key to the final focus. Upstream of these quadrupoles, a combination of bending magnets that disperse the beam combined with nonlinear sextupole magnets ensures that higher energy particles get a bit *more* focusing than lower energy particles. When a bunch arrives at the last quadrupole, the chromatic effect of the magnetic field upon it is exactly canceled.

The basic principles of the chromatic correction for particle beams have been known and utilized for about 30 years. Their first application in a linear collider was in the SLC, where the beams are demagnified by about a factor of 30, yielding spot sizes of about two microns. Because the demagnification necessary in the NLC is about a factor of 300, however, the design of its final focus system will be substantially different from that of the SLC.

4.8. The FFTB Project

In order to test such a next-generation final focus experimentally, an international collaboration including SLAC, INP, KEK, Orsay, DESY and NPI has been formed to design and construct a Final Focus Test Beam (FFTB) at SLAC.²⁵ This facility will use the SLC beam emerging straight ahead from the linac as its source of electron bunches.

Figure 15 shows a schematic of the location and layout of the FFTB. It is a scaled version of an NLC final focus, and as such, is qualitatively similar to NLC designs. A special feature of the design is that the chromaticity-correcting sextupoles are grouped in separate pairs, one for the horizontal dimension and one for the vertical. This pair of magnets is arranged so that the nonlinear aberrations introduced are cancelled, while the chromatic effects add. The bends shown in Fig. 15 horizontally disperse the different momenta in the beam so that the sextupoles give somewhat more focusing to the higher-energy particles. This additional focusing is arranged so as to cancel the lack of focusing of the higher-energy particles in the final quadrupoles.

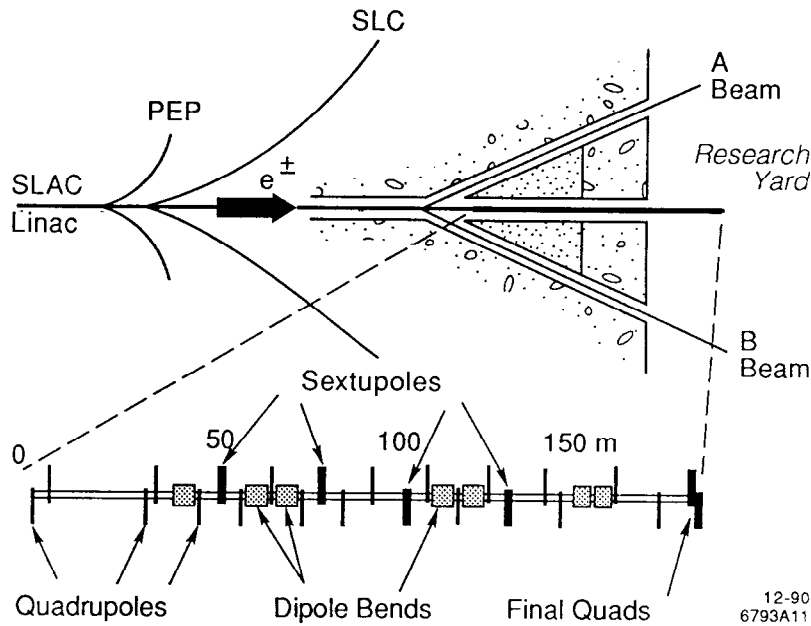


Fig. 15. The location and schematic layout of the Final Focus Test Beam.

The goal of the FFTB is to produce bunches with transverse dimensions of 60 nanometers high by 1 micron wide. Figure 16 shows the vertical beam size plotted versus the vertical β^* at the IP. In an ideal linear system, as discussed in

Section 4.3, the beam size is just proportional to the square root of β^* . This is shown as the dotted line in Fig. 16. If the bunch has finite energy spread and with no correction, this linear decrease is modified by chromatic aberrations so that the beam size reaches a minimum of about 1 μm (the solid line in Fig. 16). Finally, if the chromatic-correction sextupoles are powered and if the system is properly tuned and adjusted, the vertical beam size follows the linear optics down to a size of about 60 nm before other high-order effects spoil the compensation (the dashed line in Fig. 16).

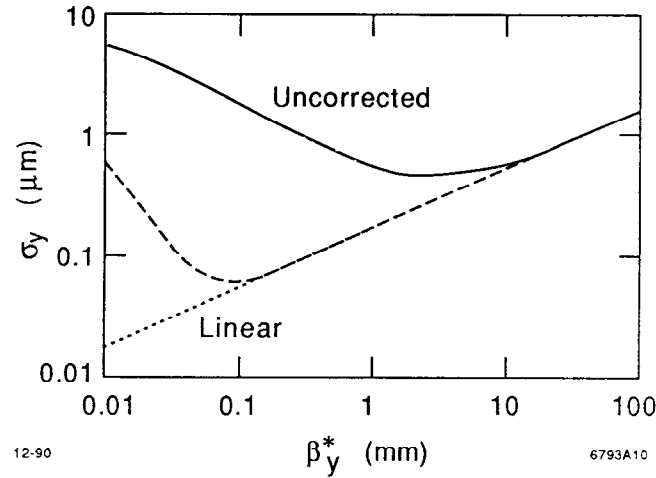


Fig. 16. Beam size versus optical tuning for uncorrected optics (solid), corrected optics (dashed) and linear optics (dotted).

The FFTB will not achieve the beam size necessary for NLC due to the lack of a suitable low-emittance source. In fact, to achieve such low emittance, we need the NLC damping ring and linac. The FFTB *will*, however, test the optical demagnification necessary for an NLC. In fact, the design β^* for FFTB is identical to that for NLC. In addition to this primary goal, the collaboration will use this facility to test the alignment, stability and instrumentation requirements needed to achieve such small spots. The FFTB project is proceeding on schedule. Most of the magnets have been received and measured and initial tests of the first part of the beam line have just been completed. The initial tests of the FFTB should begin in 1993.

4.9. Collimation and Final Focus Layout

Perhaps one of the most important lessons learned from the SLC is that it is necessary to carefully collimate the beam to eliminate background in the detector.

Unfortunately, the collimation process can dilute the emittance of the beam if done in the usual manner. In addition, if the beam is missteered the collimator can be destroyed on a single pulse of the linac. To avoid both of these problems, a nonlinear collimation section has been developed at SLAC.²⁶ This technique uses nonlinear magnets to blow up the tails of the beam for easier collimation while leaving the core unaffected. These magnets also protect the collimators by dispersing the beam if it is missteered, which eliminates collimator damage.

The collimation section also creates a beam of muons, which shine straight ahead of the section. In order to avoid background in the detector due to these muons, it is probably necessary to provide a 10-mrad-low field bend after the collimation section.

Taking all this together, the layout of the NLC after the linac takes the form shown in Fig. 17. At the end of the linac the beam is matched into the collimation section. A rather long (but necessary) collimation section serves for both transverse phase space and momentum spread collimation. The beam is matched into the big bend and is bent away from the muon beam. Finally, the beam is matched into the final focus and focused into a small spot for collisions.

4.9. Beam-Beam Effects²⁷⁻³²

When two oppositely-charged bunches collide at the IP, the intense electromagnetic field generated by the bunches tends to mutually focus them. This leads to disruption of the bunch and to a pinch enhancement of the luminosity. The enhancement factor H_D was given in Eq. 1 for the luminosity. For round bunches, this enhancement can be quite large ($\gtrsim 5$); for flat bunches, however, it is considerably reduced ($\lesssim 2$) because the pinch only occurs in one dimension. If, in addition, the bunches are misaligned relative to each other, the centroids are attracted during the bunch passage. This leads to a two-stream instability which for moderate disruption actually helps the collision process; if the bunches are misaligned, they bend toward each other and collide partially anyway.

The combination of very high electromagnetic fields and high particle energy yields substantial amounts of synchrotron radiation known as beamstrahlung. The average energy loss due to beamstrahlung ranges from 1 to 20 percent in various NLC designs. In extreme cases, many of these photons can subsequently generate electron-positron pairs in the intense electromagnetic fields present. The radiated photons or charged particles can strike detector components, causing undesirable backgrounds.

The train of bunches on each cycle also presents a problem at the final focus. In order to have a separate channel for the outgoing disrupted bunch, collisions take place at a small angle. As the bunches approach the collision point, they feel the field from those bunches which are exiting and have already collided. This sequence of bunches can induce a multibunch kink instability which can cause trailing bunches

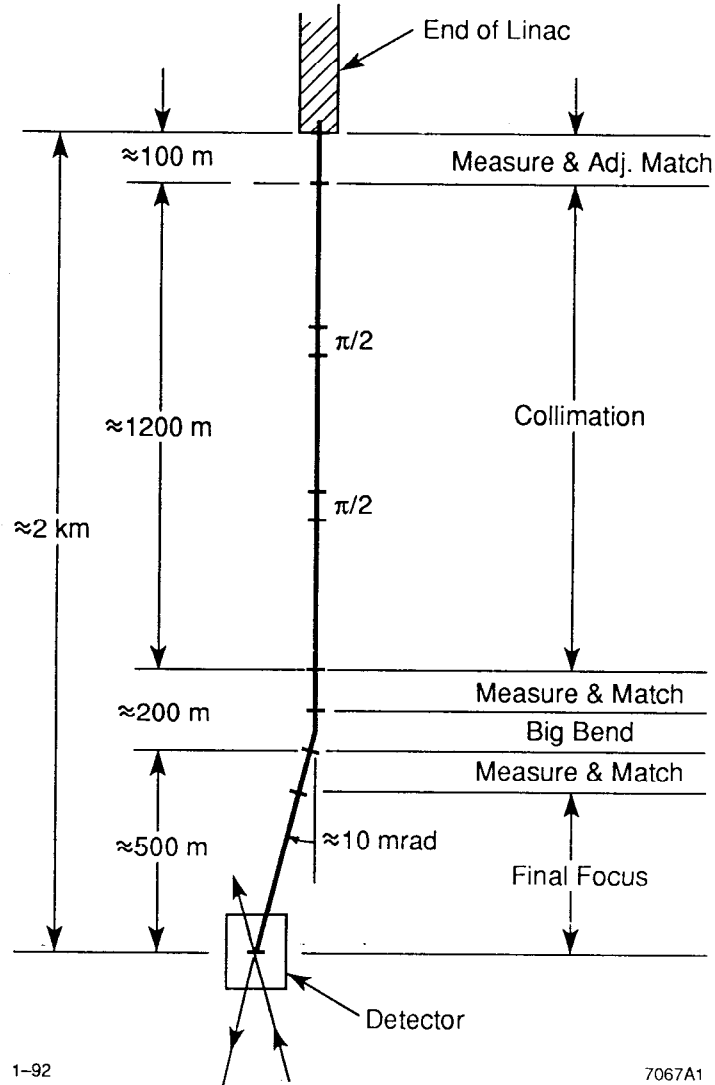


Fig. 17. Layout of the NLC final focus with collimation section.

to miss the interaction point. This effect can be controlled by the charge per bunch or by the crossing angle.

In practice, these beam-beam effects are what impose the ultimate limits on the possible charge per bunch—and thus on the luminosity. In the design described above, the luminosity limit is bypassed by using a short train of bunches, each with moderate total charge. This approach allows us to maintain the desired luminosity while keeping beam-beam effects under control.

Recently, questions have been raised regarding the background due to $\gamma + \gamma \rightarrow$ jets where the γ 's are produced by beamstrahlung.³³ Because of the large cross section, there can be more than one event per crossing in many designs. Recent

estimates suggest that although this may not be serious at 0.5 TeV, it will definitely be a problem at 1 TeV.³⁴ This effect will push designs towards more bunches per cycle with less charge per bunch. However, there are tradeoffs between detector design and linear collider design which have yet to be explored to help solve this problem.

5. Outlook

There has been a tremendous amount of progress in the accelerator physics and technology of linear colliders during the past five years. This has come from a combination of experience with the SLC, and research and development around the world. The NLC design at SLAC has evolved towards more conservative parameters, taking into account the real experience with the SLC. We are very close to having the key components of the technology under our belt, an NLC-style final focus with the FFTB and a model of the high-gradient linac, the NLC Test Accelerator. The ATF at KEK will provide a test of the next generation of damping rings. The SLC will continue to provide us with useful information about a real working linear collider. In addition, the SLC provides a test bed to perform scaled experiments to test our understanding of the accelerator physics necessary to obtain the luminosity.

A key question is: can we accelerate flat, low-emittance beams while preserving their emittance? We believe the answer is yes, but experiments on the SLC which probe our understanding of this question are essential. The final boost of a factor of 10 in luminosity is obtained by accelerating 10 bunches on each machine cycle. The choice of multiple bunches impacts every system of the collider. Although we believe we have solved all the key problems associated with the multi-bunch issue, there is a significant risk remaining with this approach. Because of this risk, we feel it is important to be able to achieve the design luminosity with only very few bunches. Our understanding of beam-beam effects and how they effect backgrounds has improved; however, much more work needs to be done on the interaction of backgrounds, detector design and collider design.

To conclude, during the next few years we look forward to the resolution of both the technical and accelerator physics issues important to the design of the Next Linear Collider.

References

1. R.D. Ruth, "The Next Linear Collider," *Proc. of the 18th SLAC Summer Institute on Particle Physics*, Stanford, CA (1990), SLAC-Report-378; *Proc. of the US-CERN School on Particle Accelerators*, Hilton Head, SC (1990); and in SLAC-PUB-5406.
2. J.T. Seeman, "The Stanford Linear Collider," *Ann. Rev. of Nucl. and Part. Sci.*, **41** (1991) 389, and in SLAC-PUB-5607; see also references quoted therein.

3. H. Deruyter *et al.*, "Damped Accelerator Structures," *Proc. of the 2nd European Part. Acc. Conf.*, Nice, France (1990).
4. J. Wang *et al.*, "Wakefield Measurements of SLAC Linac Structures at the Argonne ATF," *Proc. of the 1991 IEEE Part. Acc. Conf.*, San Francisco, CA (1991), and in SLAC-PUB-5498.
5. K. Bane and R. Gluckstern, to be published.
6. Z.D. Farkas, "Binary Peak Power Multiplier and its Application to Linear Accelerator Design," *IEEE Transcripts on Microwave Theory and Techniques*, MTT-34 No. 10 (1986) 1036, and in SLAC-PUB-3694.
7. T.L. Lavine *et al.*, "Binary RF Pulse Compression Experiment at SLAC," *Proc. of the 2nd European Part. Acc. Conf.*, Nice, France (1990), and in SLAC-PUB-5277.
8. P.B. Wilson, Z.D. Farkas and R.D. Ruth, "SLED-II: A New Method of RF Pulse Compression," *Proc. of the Linear Acc. Conf.*, Albuquerque, NM (1990), and in SLAC-PUB-5330.
9. A.E. Vlieks *et al.*, "100 MW Klystron Development at SLAC," *Proc. of the 1991 IEEE Part. Acc. Conf.*, San Francisco, CA (1991), and in SLAC-PUB-5480.
10. R. Cassel, private communication.
11. E.D. Courant and H.S. Snyder, "Theory of the Alternating-Gradient Synchrotron," *Ann. of Phys.* **3**, 1 (1958).
12. T.O. Raubenheimer, L.Z. Rivkin and R.D. Ruth, "Damping Ring Designs for a TeV Linear Collider" *Proc. of 1988 DPF Summer Study*, Snowmass, CO (1988) 620, and in SLAC-PUB-4808.
13. T.O. Raubenheimer *et al.*, "A Damping Ring Design for Future Linear Colliders," *Proc. of 1989 IEEE Part. Acc. Conf.*, Chicago, IL (1989) 1316, and in SLAC-PUB-4912.
14. S.A. Kheifets, R.D. Ruth, J.J. Murray and T.H. Fieguth, "Bunch Compression for the TLC: Preliminary Design," *Proc. of 1988 DPF Summer Study*, Snowmass, CO (1988) 632, and in SLAC-PUB-4802.
15. S.A. Kheifets, R.D. Ruth and T.H. Fieguth, "Bunch Compression for the TLC," *Proc. of Int. Conf. on High Energy Acc.*, Tsukuba, Japan (1989) and in SLAC-PUB-5034.
16. T.O. Raubenheimer and R.D. Ruth, "A Dispersion-Free Trajectory Correction Technique for Linear Colliders," *Nuc. Instr. Meth.* **A302**, 191 (1991), and in SLAC-PUB-5222.
17. T.O. Raubenheimer, "A New Technique of Correcting Emittance Dilutions in Linear Colliders," *Nuc. Instr. Meth.* **A306**, 61 (1991), and in SLAC-PUB-5355.

18. T.O. Raubenheimer, "The Generation and Acceleration of Low Emittance Flat Beams for Future Linear Colliders," Ph.D. Dissertation, and in SLAC-Report-387.
19. A. Chao, B. Richter and C. Yao, *Nucl. Instr. Meth.* **178**, 1 (1980).
20. V. Balakin, A. Novokhatsky and V. Smirnov, *Proc. of the 12th Int. Conf. on High Energy Accelerators*, Batavia, IL (1983) 119.
21. K. Oide, "Final Focus System for TLC," *Proc. of 1988 DPF Summer Study*, Snowmass, CO (1988) 665, and in SLAC-PUB-4806.
22. J. Irwin, "The Applications of Lie Algebra Techniques to Beam Transport Design," *Nucl. Inst. & Meth.*, **A298** (1990) 460, and in SLAC-PUB-5315.
23. J.J. Murray, K.L. Brown and T.H. Fieguth, "The Completed Design of the SLC Final Focus System," *Proc. of the 1989 Part. Acc. Conf.*, (1987) 331, and SLAC-PUB-4219.
24. K. Oide, "Synchrotron Radiation Limit on the Focusing of Electron Beams," *Phys. Rev. Lett.*, **61** (1988) 1713.
25. J. Buon, "Final Focus Test Beam for the Next Linear Collider," *Proc. of the 2nd European Part. Acc. Conf.*, Nice, France (1990).
26. N. Merminga, J. Irwin, R. Helm and R.D. Ruth, "Collimation Systems for a TeV Linear Collider," submitted to *Nucl. Inst. Meth. A*, and in SLAC-PUB-5165 (1992).
27. P. Chien, "Disruption, Beamstrahlung, and Beamstrahlung Pair Creation," *Proc. of 1988 DPF Summer Study*, Snowmass, CO (1988) 673, and in SLAC-PUB-4822.
28. R. Blankenbecler, S.D. Drell and N. Kroll, "Pair Production From Photon Pulse Collisions," *Phys. Rev. D*, **40** (1989) 2462, and in SLAC-PUB-4954.
29. P. Chen and V.I. Telnov, "Coherent Pair Creation in Linear Colliders," *Phys. Rev. Lett.*, **63** (1989) 1796, and in SLAC-PUB-4923.
30. M. Jacob and T.T. Wu, "Pair Production in Bunch Crossing," *Phys. Lett. B*, **221** (1989) 203.
31. V.N. Baier, V.M. Katkov and V.M. Strakhovenko, *Proc. 14th International Conf. on High Energy Particle Accelerators*, Tsukuba, Japan (1989).
32. M.S. Zolotarev, E.A. Kuraev and V.G. Serbo, "Estimates of Electromagnetic Background Processes for the VLEPP Project," Inst. Yadernoi Fiziki, Preprint 81-63 (1981), English Translation SLAC TRANS-0227 (1987).
33. M. Drees and R. Godbole, "Minijets and Large Hadronic Backgrounds at e^+e^- Supercolliders," *Phys. Rev. Lett.*, **67** 1189 (1991).
34. P. Chen, J. Bjorken, M. Peskin and S. Brodsky, to be published.